J. Phys.: Condens. Matter **11** (1999) 9403–9419. Printed in the UK PII: S0953-8984(99)06220-7

Theory of interlayer exchange interactions in magnetic multilayers

P Bruno

Max-Planck-Institut für Mikrostrukturphysik, Weinberg 2, D-06120 Halle, Germany

E-mail: bruno@mpi-halle.de

Received 21 July 1999

Abstract. This paper presents a review of the phenomenon of interlayer exchange coupling in magnetic multilayers. The emphasis is put on a pedagogical presentation of the mechanism of the phenomenon, which has been successfully explained in terms of a spin-dependent quantum confinement effect. The theoretical predictions are discussed in connection with corresponding experimental investigations.

1. Introduction

Since the first observation by Grünberg *et al* [1] of antiferromagnetic coupling of Fe films separated by a Cr spacer, the interlayer exchange interaction between ferromagnetic layers separated by a non-magnetic spacer has been a subject of intense research, in particular in the last few years. The decisive stimulus came from the discovery, by Parkin *et al* [2], of *oscillations* of the interlayer exchange coupling in Fe/Cr/Fe and Co/Ru/Co multilayers, as a function of spacer thickness. Furthermore, Parkin [3] showed that this spectacular phenomenon occurs with almost any metal as the spacer material.

This review will be restricted to the case of interlayer coupling across non-magnetic metallic spacer layers. This excludes the cases of non-metallic spacers [4–9], of antiferromagnetic spacers such as Cr or Mn [10–21], and of rare-earth multilayers [22–25]. This choice is motivated by the fact that the physical mechanism of the coupling in these cases is quite different from the one to be discussed here.

The magnetic coupling energy per unit area can usually be expressed as

$$E(\theta) = J\cos\theta \tag{1}$$

where θ is the angle between the magnetizations of the two magnetic layers, and J is called the interlayer-coupling coupling constant. Higher-order terms in an expansion in powers of $\cos\theta$ are also observed; such terms, which give rise to non-collinear alignment of the magnetizations, are believed to be of non-intrinsic origin and to be related to defects such as roughness [26, 27]. Such effects will not be considered here. In addition, due to space limitations, the important question of the role of alloy disorder and interdiffusion [28–31] will not be addressed.

The purpose of this paper is to present as simply as possible the mechanism of interlayer exchange coupling in terms of quantum interferences due to electron confinement in the spacer layer. The understanding of this mechanism relies on ideas due to various authors [32–36]. The presentation given here is based on that of reference [36]. The emphasis will be on

0953-8984/99/489403+17$30.00

physical concepts and pedagogical clarity rather than on mathematical rigour. It is organized as follows: in the next section, an elementary discussion of quantum confinement is given; in section 3, it is then shown how spin-dependent confinement in the spacer layer gives rise to interlayer exchange coupling; section 4 is devoted to the limit of large spacer thicknesses, for which particularly simple results are obtained; sections 5 and 6 treat the variation of interlayer exchange coupling with magnetic layer thickness and non-magnetic overlayer thickness, respectively; finally, in section 7 the strength of the interlayer exchange coupling is discussed in comparison with experimental data.

The point of view adopted here reflects the author's subjective views on the topic. In particular, due to space limitations, the important literature devoted to *ab initio* calculation will not be discussed in detail here. The interested reader can find complementary information in the various review papers on this subject which have been published recently [26, 37–42].

2. Elementary discussion of quantum confinement

For the sake of clarity, we shall first consider an extremely simplified model, namely the one-dimensional quantum well, which nevertheless contains the essential physics involved in the problem. Then, we shall progressively refine the model in order to make it more realistic.

The model consists in a one-dimensional quantum well representing the spacer layer (of potential $V = 0$ and width D), sandwiched between two 'barriers' A and B of respective widths L_A and L_B, and respective potentials V_A and V_B. Note that we use the term 'barrier' in a general sense, i.e., V_A and V_B are not necessarily positive. Furthermore, the barrier widths, L_A and L_B, can be finite or infinite, without any restriction.

2.1. Change of the density of states due to quantum interferences

Let us consider an electron of wavevector k^+ (with $k^+ > 0$) propagating towards the right in the spacer layer; as this electron arrives at barrier B, it is partially reflected to the left, with a (complex) amplitude $r_B \equiv |r_B|e^{i\phi_B}$. The reflected wave of wavevector k^- is in turn reflected at barrier A with an amplitude $r_A \equiv |r_A|e^{i\phi_A}$, an so on†. The modulus $|r_{A\,(B)}|$ of the reflection coefficient expresses the magnitude of the reflected wave, whereas the argument $\phi_{A\,(B)}$ represents the phase shift due to the reflection (note that the latter is not absolutely determined and depends on the choice of the coordinate origin).

The interferences between the waves due to the multiple reflections at the barriers induce a modification of the density of states in the spacer layer, for the electronic state under consideration. The phase shift resulting from a complete round trip in the spacer is

$$\Delta\phi = qD + \phi_A + \phi_B \tag{2}$$

with

$$q \equiv k^+ - k^-. \tag{3}$$

If the interferences are constructive, i.e., if

$$\Delta\phi = 2n\pi \tag{4}$$

with n an integer, one has an increase of the density of states; conversely, if the interferences are destructive, i.e., if

$$\Delta\phi = (2n+1)\pi \tag{5}$$

† Of course, for the one-dimensional model, one has $k^- = -k^+$; however, this property will generally not hold for three-dimensional systems, to be studied below.

one has a reduction of the density of states. Thus, in a first approximation, we expect the modification of the density of states in the spacer, $\Delta n(\varepsilon)$, to vary with D like

$$\Delta n(\varepsilon) \approx \cos(qD + \phi_A + \phi_B). \tag{6}$$

Furthermore, we expect this effect to be proportional to the amplitude of the reflections at barriers A and B, i.e., to $|r_A r_B|$; finally, $\Delta n(\varepsilon)$ must be proportional to the width D of the spacer and to the density of states per unit energy and unit width:

$$\frac{2}{\pi}\frac{\mathrm{d}q}{\mathrm{d}\varepsilon} \tag{7}$$

which includes a factor of 2 for spin degeneracy. We can also include the effect of higher-order interferences due to n round trips in the spacer; the phase shift $\Delta\phi$ is then multiplied by n and $|r_A r_B|$ is replaced by $|r_A r_B|^n$. Gathering all the terms, we get

$$\begin{aligned}\Delta n(\varepsilon) &\approx \frac{2D}{\pi}\frac{\mathrm{d}q}{\mathrm{d}\varepsilon}\sum_{n=1}^{\infty}|r_A r_B|^n \cos n(qD + \phi_A + \phi_B) \\ &= \frac{2}{\pi}\,\mathrm{Im}\left(\mathrm{i}D\frac{\mathrm{d}q}{\mathrm{d}\varepsilon}\sum_{n=1}^{\infty}(r_A r_B)^n \mathrm{e}^{n\mathrm{i}qD}\right) = \frac{2}{\pi}\,\mathrm{Im}\left(\mathrm{i}\frac{\mathrm{d}q}{\mathrm{d}\varepsilon}\frac{r_A r_B \mathrm{e}^{\mathrm{i}qD}}{1 - r_A r_B \mathrm{e}^{\mathrm{i}qD}}\right).\end{aligned} \tag{8}$$

As will appear clearly below, it is more convenient to consider the integrated density of states

$$N(\varepsilon) \equiv \int_{-\infty}^{\varepsilon} n(\varepsilon')\,\mathrm{d}\varepsilon'. \tag{9}$$

The modification $\Delta N(\varepsilon)$ of the integrated density of states due to electron confinement is

$$\Delta N(\varepsilon) = \frac{2}{\pi}\,\mathrm{Im}\sum_{n=1}^{\infty}\frac{(r_A r_B)^n}{n}\mathrm{e}^{n\mathrm{i}qD} = -\frac{2}{\pi}\,\mathrm{Im}\ln(1 - r_A r_B \mathrm{e}^{\mathrm{i}qD}). \tag{10}$$

A simple graphical interpretation of the above expression can be obtained by noting that $\mathrm{Im}\ln(z) = \mathrm{Arg}(z)$, for z complex; thus, $\Delta N(\varepsilon)$ is given by the argument, in the complex plane, of a point located at an angle $\Delta\phi = qD + \phi_A + \phi_B$ on a circle of radius $|r_A r_B|$ centred at 1. This graphical construction is shown in figure 1.

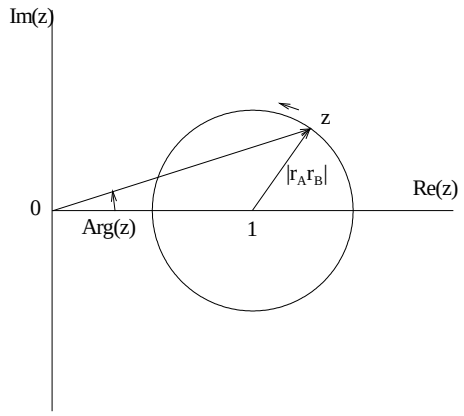

Figure 1. Graphical interpretation of equation (10).

The variation of $\Delta N(\varepsilon)$ as a function of D is shown in figure 2, for various values of the confinement strength $|r_A r_B|$. For weak confinement, figure 2(a), $\Delta N(\varepsilon)$ varies with D in a

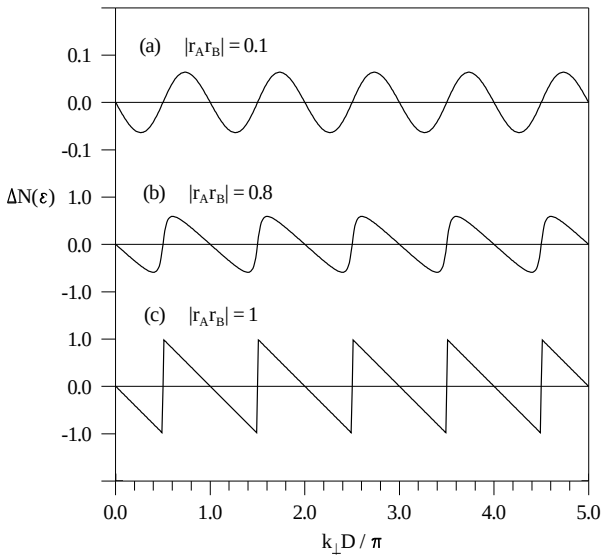

Figure 2. Variation of $\Delta N(\varepsilon)$ as a function of D, for various values of the confinement strength: (a) $|r_A r_B| = 0.1$, (b) $|r_A r_B| = 0.8$, (c) $|r_A r_B| = 1$ (full confinement). Note the different scales along the ordinate axis.

sinusoidal manner. As one increases the confinement strength, figure 2(b), the oscillations are distorted, due to higher-order interferences. Finally, for full confinement, figure 2(c), $\Delta N(\varepsilon)$ exhibits some jumps that correspond to the appearance of bound states. We note, however, that the period Λ of the oscillations of $\Delta N(\varepsilon)$ depends not on the confinement strength, but only on the wavevector $q \equiv k^+ - k^-$; that is, $\Lambda = 2\pi/q$.

So far, we have implicitly restricted consideration to positive-energy states. Negative-energy states (i.e., of imaginary wavevector) are forbidden in the absence of the barriers A and B, because their amplitude diverges either on the right-hand side or on the left-hand side, so they cannot be normalized. This no longer holds in the presence of the barriers if V_A (or V_B, or both V_A and V_B) is negative: the negative-energy states, i.e., ones varying exponentially in the spacer, can be connected to allowed states of A or B. In order to treat these states consistently, we simply have to extend the concept of the reflection coefficient to states of imaginary wavevector, which is straightforward. One can check that, with this generalization, equation (10) accounts properly for the contribution of the evanescent states. Physically, this can be interpreted as a coupling of A and B by the tunnel effect [7, 36].

2.2. Energy associated with the quantum interferences in the spacer

Let us now study the modification of the energy of the system due to the quantum interferences. In order to conserve the total number of electrons, it is convenient to work within the grand-canonical ensemble, and to consider the thermodynamic grand potential, which is given by

$$\Phi \equiv -k_B T \int_{-\infty}^{+\infty} \ln\left[1 + \exp\left(\frac{\varepsilon_F - \varepsilon}{k_B T}\right)\right] n(\varepsilon)\, \mathrm{d}\varepsilon = -\int_{-\infty}^{+\infty} N(\varepsilon) f(\varepsilon)\, \mathrm{d}\varepsilon. \tag{11}$$

At $T = 0$, this reduces to

$$\Phi \equiv \int_{-\infty}^{\varepsilon_F} (\varepsilon - \varepsilon_F) n(\varepsilon)\, \mathrm{d}\varepsilon = -\int_{-\infty}^{\varepsilon_F} N(\varepsilon)\, \mathrm{d}\varepsilon. \tag{12}$$

The energy ΔE associated with the interferences is the contribution to Φ corresponding to $\Delta N(\varepsilon)$:

$$\Delta E = \frac{2}{\pi} \operatorname{Im} \int_{-\infty}^{+\infty} \ln(1 - r_A r_B e^{iqD})\, d\varepsilon. \tag{13}$$

2.3. The three-dimensional layered system

The generalization of the above discussion to the more realistic case of a three-dimensional layered system is immediate. Since the system is invariant on translation parallel to the plane, the in-plane wavevector $\boldsymbol{k}_\parallel$ is a good quantum number. Thus, for a given $\boldsymbol{k}_\parallel$, one has an effective one-dimensional problem analogous to the one discussed above. The resulting effect of quantum interferences is obtained by summing over $\boldsymbol{k}_\parallel$ over the two-dimensional Brillouin zone. The modification of the integrated density of states per unit area is

$$\Delta N(\varepsilon) = -\frac{1}{2\pi^3} \operatorname{Im} \int d^2\boldsymbol{k}_\parallel \ \ln(1 - r_A r_B e^{iq_\perp D}) \tag{14}$$

and the interference energy per unit area is

$$\Delta E = \frac{1}{2\pi^3} \operatorname{Im} \int d^2\boldsymbol{k}_\parallel \int_{-\infty}^{+\infty} f(\varepsilon) \ln(1 - r_A r_B e^{iq_\perp D})\, d\varepsilon. \tag{15}$$

2.4. The quantum size effect in an overlayer

The case of a thin overlayer deposited on a substrate is of considerable interest. In this case, one of the barriers (say, A) consists of the vacuum, and barrier B is constituted by the substrate itself. The potential of the vacuum barrier is $V_{vac} = \varepsilon_F + W$, where W is the work function; thus it is perfectly reflecting for occupied states, i.e., $|r_{vac}| = 1$. On the other hand, the reflection at the substrate (or coefficient r_{sub}) may be total or partial, depending on the band matching for the state under consideration.

The spectral density of the occupied states in the overlayer can be investigated experimentally by photoemission spectroscopy; in addition, by using inverse photoemission, one can study the unoccupied states. If furthermore these techniques are used in the 'angle-resolved' mode, they give information on the spectral density *locally in the $\boldsymbol{k}_\parallel$-plane*.

For a given thickness of the overlayer, the photoemission spectra (either direct or inverse) exhibit some maxima and minima corresponding, respectively, to the energies for which the interferences are constructive and destructive. When the confinement is total, narrow peaks can be observed, which correspond to the quantized confined states in the overlayer, as was pointed out by Loly and Pendry [43].

Quantum size effects due to electron confinement in the photoemission spectra of overlayers have been observed in various non-magnetic systems [44–52]. In particular, the systems Au(111)/Ag/vacuum and Cu(111)/Ag/vacuum offer excellent examples of this phenomenon [49, 51].

2.5. A paramagnetic overlayer on a ferromagnetic substrate: the spin-polarized quantum size effect

So far our discussion has concerned exclusively non-magnetic systems. Qualitatively new behaviour can be expected when some of the layers are ferromagnetic. A case of particular interest is that of a paramagnetic overlayer on a ferromagnetic substrate.

In the interior of the overlayer, the potential is independent of the spin; therefore the propagation of electrons is described by a wavevector $k_\perp$ which is spin independent. The

coefficient of reflection at the vacuum barrier, $r_{\rm vac}$, is also spin independent. However, the ferromagnetic substrate constitutes a spin-dependent potential barrier; thus, the substrate reflection coefficients for electrons with spin parallel to the majority- and minority-spin directions of the substrate, respectively $r_{\rm sub}^{\uparrow}$ and $r_{\rm sub}^{\downarrow}$, are different. It is convenient to define the spin average

$$\overline{r}_{\rm sub} \equiv \frac{r_{\rm sub}^{\uparrow} + r_{\rm sub}^{\downarrow}}{2} \tag{16}$$

and the spin asymmetry

$$\Delta r_{\rm sub} \equiv \frac{r_{\rm sub}^{\uparrow} - r_{\rm sub}^{\downarrow}}{2}. \tag{17}$$

In this case, the electron confinement in the overlayer gives rise to a spin-dependent modulation of the spectral density versus overlayer thickness; the period of the modulation is the same for the two spins, whereas the amplitude and phase are expected to be spin dependent.

The quantum size effects in paramagnetic overlayers on a ferromagnetic substrate have been investigated by several groups [53–66]. The systems studied most are Cu overlayers on a Co(001) substrate and Ag overlayers on an Fe(001) substrate. Ortega and Himpsel [54, 55] observed a quantum size effect in the normal-emission photoelectron spectra of a copper overlayer on a fcc cobalt (001) substrate. They observed peaks due to quantum size effects both in the photoemission and in the inverse-photoemission spectra. These quantum size effects manifest themselves also in an oscillatory behaviour of the photoemission intensity at the Fermi level; as the observed oscillation period (5.9 atomic layers (AL)) is close to the long period of interlayer exchange-coupling oscillations in Co/Cu(001)/Co, they suggested that the two phenomena should be related to each other; they also claimed that the observed oscillations in photoemission are spin dependent and due mostly to minority electrons. A direct confirmation of this conjecture has been given independently by Garrison *et al* [57] and by Carbone *et al* [58] by means of spin-polarized photoemission. They found that both the intensity and the spin polarization exhibit oscillatory behaviours, with the same period (5–6 atomic layers), but opposite phases, which indicates that the quantum size effect does indeed take place predominantly in the minority-spin band as proposed by Ortega and Himpsel [54, 55]. Recently, Kläsges *et al* [64] and Kawakami *et al* [66] have observed spin-polarized quantum size effects in a copper overlayer on cobalt (001) for a non-zero in-plane wavevector corresponding to the short-period oscillation of the interlayer exchange coupling in Co/Cu(001)/Co; they observed short-period oscillations of the photoemission intensity in good agreement with the short-period oscillations of the interlayer coupling. This observation provides a further confirmation of the relation between quantum size effects in photoemission and oscillation of interlayer exchange coupling.

Photoemission studies of quantum size effects have also been performed for other kinds of system such as a ferromagnetic overlayer on a non-magnetic substrate, or systems comprising more layers [67–71].

Photoemission spectroscopy undoubtedly constitutes the method of choice for investigating quantum size effects in metallic overlayers: this is due to its unique features, which allow selectivity in energy, in-plane wavevector, and spin.

Besides photoemission, spin-polarized quantum size effects in paramagnetic overlayers on a ferromagnetic substrate are also responsible for the oscillatory behaviour (versus overlayer thickness) of the spin-polarized secondary-electron emission [72, 73], linear [74–79] and non-linear [80, 81] magneto-optical Kerr effect, and magnetic anisotropy [82, 83]. However, these effects usually involve a summation over all electronic states, so the quantitative analysis of the quantum size effects may be fairly complicated.

3. Interlayer exchange coupling due to quantum interferences

Let us now consider the case of a paramagnetic layer sandwiched between two ferromagnetic layers A and B. Now, the reflection coefficients on both sides of the paramagnetic spacer layer are spin dependent. *A priori*, the angle θ between the magnetizations of the two ferromagnetic layers can take any value; however, for the sake of simplicity, we shall restrict ourselves here to the ferromagnetic (F) configuration (i.e., $\theta = 0$) and the antiferromagnetic (AF) one (i.e., $\theta = \pi$).

For the ferromagnetic configuration, the energy change per unit area due to quantum interference is easily obtained from (15), i.e.,

$$\Delta E_F = \frac{1}{4\pi^3}\,\mathrm{Im}\int \mathrm{d}^2\boldsymbol{k}_\parallel \int_{-\infty}^{+\infty} f(\varepsilon)\left[\ln(1 - r_\mathrm{A}^\uparrow r_\mathrm{B}^\uparrow \mathrm{e}^{\mathrm{i}q_\perp D}) + \ln(1 - r_\mathrm{A}^\downarrow r_\mathrm{B}^\downarrow \mathrm{e}^{\mathrm{i}q_\perp D})\right]\,\mathrm{d}\varepsilon. \tag{18}$$

In this equation, the first and the second term correspond respectively to majority- and minority-spin electrons. The antiferromagnetic configuration is obtained by reversing the magnetization of B, i.e., by interchanging $r_\mathrm{B}^\uparrow$ and $r_\mathrm{B}^\downarrow$; thus the corresponding energy per unit area is

$$\Delta E_{AF} = \frac{1}{4\pi^3}\,\mathrm{Im}\int \mathrm{d}^2\boldsymbol{k}_\parallel \int_{-\infty}^{+\infty} f(\varepsilon)\left[\ln(1 - r_\mathrm{A}^\uparrow r_\mathrm{B}^\downarrow \mathrm{e}^{\mathrm{i}q_\perp D}) + \ln(1 - r_\mathrm{A}^\downarrow r_\mathrm{B}^\uparrow \mathrm{e}^{\mathrm{i}q_\perp D})\right]\,\mathrm{d}\varepsilon. \tag{19}$$

Thus, the interlayer exchange-coupling (IEC) energy is

$$E_F - E_{AF} = \frac{1}{4\pi^3}\,\mathrm{Im}\int \mathrm{d}^2\boldsymbol{k}_\parallel \int_{-\infty}^{+\infty} f(\varepsilon)\ln\left[\frac{(1 - r_\mathrm{A}^\uparrow r_\mathrm{B}^\uparrow \mathrm{e}^{\mathrm{i}q_\perp D})(1 - r_\mathrm{A}^\downarrow r_\mathrm{B}^\downarrow \mathrm{e}^{\mathrm{i}q_\perp D})}{(1 - r_\mathrm{A}^\uparrow r_\mathrm{B}^\downarrow \mathrm{e}^{\mathrm{i}q_\perp D})(1 - r_\mathrm{A}^\downarrow r_\mathrm{B}^\uparrow \mathrm{e}^{\mathrm{i}q_\perp D})}\right]\,\mathrm{d}\varepsilon \tag{20}$$

which can be simplified as

$$E_F - E_{AF} \approx -\frac{1}{\pi^3}\,\mathrm{Im}\int \mathrm{d}^2\boldsymbol{k}_\parallel \int_{-\infty}^{\infty} f(\varepsilon)\,\Delta r_\mathrm{A}\,\Delta r_\mathrm{B}\,\mathrm{e}^{\mathrm{i}q_\perp D}\,\mathrm{d}\varepsilon \tag{21}$$

in the limit of weak confinement. The above expression for the IEC has a rather transparent physical interpretation. First, as the integrations over $\boldsymbol{k}_\parallel$ over the first two-dimensional Brillouin zone and over the energy up to the Fermi level show, the IEC is a sum of contributions from all occupied electronic states. The contribution of a given electronic state, of energy ε and in-plane wavevector $\boldsymbol{k}_\parallel$, consists of the product of three factors: the two factors Δr_A and Δr_B express the spin asymmetry of the confinement due to the magnetic layers A and B, respectively, while the exponential factor $\mathrm{e}^{\mathrm{i}q_\perp D}$ describes the propagation through the spacer and is responsible for the interference (or quantum size) effect. Thus, this approach establishes an explicit and direct link between oscillatory IEC and quantum size effects such as are observed in photoemission.

4. Asymptotic behaviour for large spacer thicknesses

In the limit of large spacer thickness D, the exponential factor oscillates rapidly with ε and $\boldsymbol{k}_\parallel$, which leads to substantial cancellation of the contributions to the IEC due to the different electronic states. However, because the integration over energy is abruptly stopped at ε_F, states located at the Fermi level give the predominant contributions. Thus the integral over ε may be calculated by fixing all other factors to their value at ε_F, and by expanding $q_\perp \equiv k_\perp^+ - k_\perp^-$ around ε_F, i.e.,

$$q_\perp \approx q_{\perp F} + 2\frac{\varepsilon - \varepsilon_F}{\hbar v_{\perp F}^{+-}} \tag{22}$$

with

$$\frac{2}{v_{\perp F}^{+-}} \equiv \frac{1}{v_{\perp F}^{+}} - \frac{1}{v_{\perp F}^{-}}. \tag{23}$$

The integration (see reference [36] for details) yields

$$E_F - E_{AF} = \frac{1}{2\pi^3} \operatorname{Im} \int \mathrm{d}^2 \boldsymbol{k}_\parallel \, \frac{\mathrm{i}\hbar v_{\perp F}^{+-}}{D} \, \Delta r_\mathrm{A} \, \Delta r_\mathrm{B} \, \mathrm{e}^{\mathrm{i}q_{\perp F} D} F(2\pi k_B T D/\hbar v_{\perp F}^{+-}) \tag{24}$$

where

$$F(x) \equiv \frac{x}{\sinh x}. \tag{25}$$

In the above equations, $q_{\perp F}$ is a vector spanning the *complex Fermi surface*; the velocity $v_{\perp F}^{+-}$ is a combination of the group velocities at the points $(\boldsymbol{k}_\parallel, k_{\perp F}^{+})$ and $(\boldsymbol{k}_\parallel, k_{\perp F}^{-})$ of the Fermi surface.

Next, the integration over $\boldsymbol{k}_\parallel$ is performed by noting that, for large spacer thickness D, the only significant contributions arise from the neighbouring critical vectors $\boldsymbol{k}_\parallel^\alpha$ for which $q_{\perp F}$ is stationary. Around such vectors, $q_{\perp F}$ may be expanded as

$$q_{\perp F} = q_{\perp F}^\alpha - \frac{(k_x - k_x^\alpha)^2}{\kappa_x^\alpha} - \frac{(k_y - k_y^\alpha)^2}{\kappa_y^\alpha} \tag{26}$$

where the crossed terms have been cancelled by making an appropriate choice of the x- and y-axes; κ_x^α and κ_y^α are combinations of the curvature radii of the Fermi surface at $(\boldsymbol{k}_\parallel^\alpha, k_\perp^{+\alpha})$ and $(\boldsymbol{k}_\parallel^\alpha, k_\perp^{-\alpha})$.

The integral is calculated by using the stationary-phase approximation [36], and one obtains

$$E_F - E_{AF} = \operatorname{Im} \sum_\alpha \frac{\hbar v_\perp^\alpha \kappa_\alpha}{2\pi^2 D^2} \, \Delta r_\mathrm{A}^\alpha \, \Delta r_\mathrm{B}^\alpha \, \mathrm{e}^{\mathrm{i}q_\perp^\alpha D} F(2\pi k_B T D/\hbar v_\perp^\alpha) \tag{27}$$

where $q_\perp^\alpha$, $v_\perp^\alpha$, $\Delta r_\mathrm{A}^\alpha$, $\Delta r_\mathrm{B}^\alpha$ correspond to the critical vector $\boldsymbol{k}_\parallel^\alpha$, and

$$\kappa_\alpha \equiv (\kappa_x^\alpha)^{1/2} (\kappa_y^\alpha)^{1/2}. \tag{28}$$

In the above equation, one takes the square root with an argument between 0 and π.

This analysis shows that eventually the only remaining contributions in the limit of large spacer thickness D arise from the neighbourhood of states having in-plane wavevectors $\boldsymbol{k}_\parallel^\alpha$ such that the spanning vector of the Fermi surface $q_{\perp F} = k_{\perp F}^{+} - k_{\perp F}^{-}$ is stationary with respect to $\boldsymbol{k}_\parallel$ for $\boldsymbol{k}_\parallel = \boldsymbol{k}_\parallel^\alpha$, and the corresponding contribution oscillates with a wavevector equal to $q_{\perp F}^\alpha$. This selection rule was first derived in the context of the RKKY model [33]; it is illustrated in figure 3. There may be several such stationary spanning vectors and, hence, several oscillatory components; they are labelled by the index α.

The above selection rule allows one to predict the oscillation period(s) of the interlayer exchange coupling versus spacer thickness just by inspecting the bulk Fermi surface of the spacer material. As regards an experimental test of these predictions, noble-metal spacer layers appear to be the best suited candidates; there are several reasons for this choice:

- Fermi surfaces of noble metals are known very accurately from de Haas–van Alphen and cyclotron resonance experiments [84];
- since only the sp band intersects the Fermi level, the Fermi surface is rather simple, and does not depart very much from a free-electron Fermi sphere;
- samples of very good quality with noble metals as a spacer layer could be prepared.

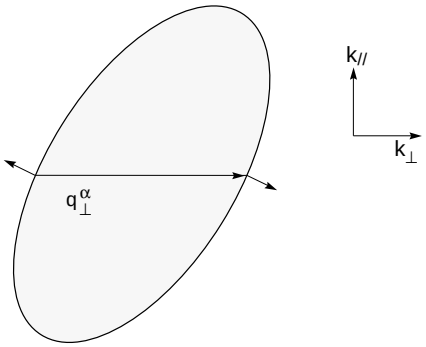

Figure 3. A sketch showing the wavevector $q_\perp^\alpha$ giving the oscillation period of the oscillatory interlayer exchange coupling, for the case of a non-spherical Fermi surface.

Figure 4 shows a cross-section of the Fermi surface of Cu, indicating the stationary spanning vectors for the (001), (111), and (110) crystalline orientations [33]; the Fermi surfaces of Ag and Au are qualitatively similar. For the (111) orientation, a single (long) period is predicted; for the (001) orientation, both a long period and a short period are predicted; for the (110) orientation, four different periods are predicted (only one stationary spanning vector is seen in figure 4, the three others being located in other cross-sections of the Fermi surface). These theoretical predictions have been confirmed successfully by numerous experimental observations. In particular, the coexistence of a long and a short period for the (001) orientation has been confirmed for Cu [40, 66, 85–87], Ag [88], and Au [89–91]; and the experimental periods have been found to be in excellent agreement with the theoretical ones. A comparison of the theoretically predicted oscillation periods and the experimentally observed ones is given in table 1.

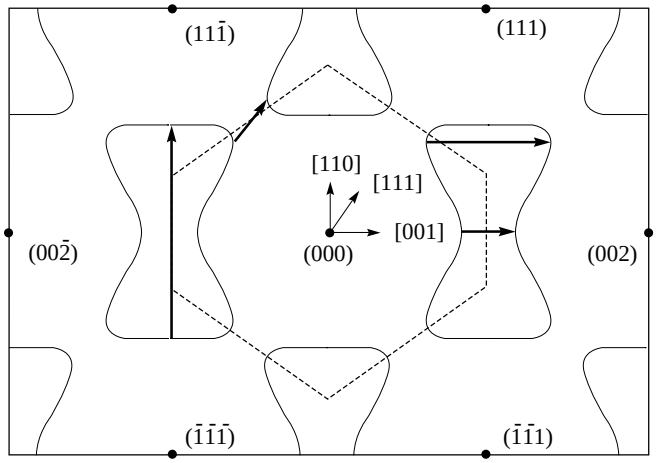

Figure 4. The cross-section of the Fermi surface of Cu along the $(1\bar{1}0)$ plane passing through the origin. The solid dots indicate the reciprocal-lattice vectors. The dashed lines indicate the boundary of the first Brillouin zone. The solid arrows, respectively horizontal, oblique, and vertical, indicate the vectors $q_\perp^\alpha$ giving the oscillation period(s) for the (001), (111), and (110) orientations.

Table 1. Comparison between the theoretical predictions of reference [33] and experimental observations for the oscillation periods of interlayer exchange coupling versus spacer thickness.

Spacer	Theory	System	Experiment	Reference
Cu(111)	$\Lambda = 4.5$ AL	Co/Cu/Co(111)	$\Lambda \approx 5$ AL	[3]
		Co/Cu/Co(111)	$\Lambda \approx 6$ AL	[92]
		Co/Cu/Co(111)	$\Lambda \approx 4.5$ AL	[93]
		Fe/Cu/Fe(111)	$\Lambda \approx 6$ AL	[94]
Cu(001)	$\Lambda_1 = 2.6$ AL $\Lambda_2 = 5.9$ AL	Co/Cu/Co(001)	$\Lambda \approx 6$ AL	[95]
		Co/Cu/Co(001)	$\Lambda_1 \approx 2.6$ AL $\Lambda_2 \approx 8$ AL	[85]
		Co/Cu/Co(001)	$\Lambda_1 \approx 2.7$ AL $\Lambda_2 \approx 6.1$ AL	[87]
		Co/Cu/Co(001)	$\Lambda_1 \approx 2.7$ AL $\Lambda_2 \approx 5.6$ AL	[66]
		Fe/Cu/Fe(001)	$\Lambda \approx 7.5$ AL	[74]
Ag(001)	$\Lambda_1 = 2.4$ AL $\Lambda_2 = 5.6$ AL	Fe/Ag/Fe(001)	$\Lambda_1 \approx 2.4$ AL $\Lambda_2 \approx 5.6$ AL	[88]
Au(001)	$\Lambda_1 = 2.5$ AL $\Lambda_2 = 8.6$ AL	Fe/Au/Fe(001)	$\Lambda_1 \approx 2$ AL $\Lambda_2 \approx 7$–8 AL	[89]
		Fe/Au/Fe(001)	$\Lambda_1 \approx 2.5$ AL $\Lambda_2 \approx 8.6$ AL	[90, 91]

In a further attempt to test the theoretical predictions for the periods of oscillatory coupling, several groups [96–98] have undertaken to modify in a controlled manner the size of the Fermi surface (and hence, the period of the coupling) by alloying the spacer noble metal (Cu) with a metal of lower valence (Ni); in all cases, the change in oscillation period due to alloying has been found to be in good agreement with the expected change in the Fermi surface.

5. The effect of magnetic layer thickness

As already mentioned, the influence of the IEC on the ferromagnetic layer thickness is contained in the reflection coefficients Δr_{A} and Δr_{B}. If the ferromagnetic layers are of finite thickness, reflections may usually take place at the two interfaces bounding the ferromagnetic layers, giving rise to interferences [99], and, hence, to oscillations of the IEC versus ferromagnetic layer thickness. A more detailed discussion of this effect is given in references [36, 99]. This behaviour was first predicted from calculations based upon a free-electron model (reference [100]). The amplitude of the oscillations of the IEC versus ferromagnetic layer thickness is generally much smaller than the oscillations versus spacer thickness, and does not give rise to changes of sign of the IEC. From the experimental point of view, this effect was confirmed by Bloemen *et al* [101] for Co/Cu/Co(001) and by Back *et al* [102] for Fe/Cu/Co(001). It has also been confirmed theoretically by Nordström *et al* [103], Lang *et al* [104], Drchal *et al* [105], and by Lee and Chang [106].

6. The effect of overlayer thickness

A more (at first sight) surprising behaviour is the dependence of the IEC on the thickness of an external overlayer. From a naïve point of view, one might think that layers external to the basic ferromagnet/spacer/ferromagnet sandwich should not influence the interaction between the two ferromagnetic layers. This view is incorrect, in particular when the system is covered by an ultrathin protective overlayer. In this case, the electrons are able to reach the vacuum barrier, which is a perfectly reflecting one, so strong confinement and interference effects take place in the overlayer, which leads to a weak but significant oscillatory variation of the IEC as a function of the overlayer thickness (reference [107]).

This effect, which follows directly from the quantum interference (or quantum size effect) mechanism, has been proposed and experimentally confirmed independently by de Vries *et al* [108] for the Co/Cu/Co(001) system with a Cu(001) overlayer, by Okuno and Inomata [109] for the Fe/Au/Fe(001) system with a Au(001) overlayer, and by Bounouh *et al* [110] for the Co/Au/Co(0001) system with a Au(111) overlayer. In all cases, the observed period(s) for the oscillations versus overlayer thickness were found to be in good agreement with the theoretically predicted ones. This effect has also been confirmed by means of first-principles calculations for the Co/Cu/Co(001) system with various types of overlayer (references [111–113]). The comparison between the periods of oscillations versus overlayer thickness predicted theoretically and those observed experimentally is given in table 2. A more detailed discussion of this effect can be found in references [107, 111, 113].

Table 2. Comparison between the theoretical predictions of reference [107] and experimental observations for the oscillation periods of the interlayer exchange coupling versus overlayer thickness.

Overlayer	Theory	System	Experiment	Reference
Cu(001)	$\Lambda_1 = 2.6$ AL $\Lambda_2 = 5.9$ AL	Cu/Co/Cu/Co/Cu(001)	$\Lambda \approx 5$ AL	[108]
Au(001)	$\Lambda_1 = 2.5$ AL $\Lambda_2 = 8.6$ AL	Au/Fe/Au/Fe/Au(001)	$\Lambda_1 \approx 2.6$ AL $\Lambda_2 \approx 8.0$ AL	[109]
Au(111)	$\Lambda = 4.8$ AL	Au/Co/Au/Co/Au(111)	$\Lambda \approx 5$ AL	[110]

7. The strength and phase of the interlayer exchange coupling

In contrast with the excellent agreement between theory and experiment which is obtained for oscillation periods, the situation for the amplitude and phase of the oscillations is less satisfactory. According to the theory presented above, the coupling takes the following form in the limit of large spacer thickness (asymptotic limit):

$$J = \sum_{\alpha} \frac{A_\alpha}{D^2} \sin(q_\alpha D + \phi_\alpha). \tag{29}$$

Since the coupling constant J has the dimension of an energy per unit area, the parameters A_α characterizing the coupling strength of the various oscillatory components have the dimension of an energy. By taking typical values of the Fermi wavevector and velocity, it is easy to see from equation (27) that they are typically of the order of 1 to 10 meV.

Table 3 presents a comparison of theoretical and experimental values of the oscillation amplitude strengths A_α, for various systems†. We observe that there is a rather strong discrepancy between theory and experiment, but also among various theoretical studies. Although the agreement seems to be rather good for the Co/Cu(111)/Co system, more experimental and theoretical data would be required in order to establish whether the apparent agreement is conclusive or accidental.

Table 3. Comparison between the theoretical predictions and experimental observations for the oscillation amplitudes A_α of the interlayer exchange coupling versus spacer thickness; for Cu(001) and Au(001) spacers, A_1 and A_2 correspond, respectively, to the short-period and long-period oscillations.

System	Theory	Reference	Experiment	Reference
Co/Cu(111)/Co	$A \approx 3.7$ meV	[114]	$A \approx 7.6$ meV	[85]
	$A \approx 4.2$ meV	[115]	$A \approx 3.4$ meV	[93]
			$A \approx 2.5$ meV	[117]
Co/Cu(001)/Co	$A_1 \approx 42$ meV	[114]	$A_1 \approx 1.6$ meV	[40, 85, 86]
	$A_2 \approx 0.13$ meV		$A_2 \approx 1.4$ meV	
	$A_1 \approx 72$ meV	[115]		
	$A_2 \approx 0.75$ meV			
	$A_1 \approx 35$ meV	[105]		
	$A_2 \approx 3.5$ meV			
	$A_1 \approx 35$ meV	[116]		
	$A_2 \approx 0.035$ meV			
Fe/Au(001)/Fe	$A_1 \approx 12.5$ meV	[115]	$A_1 \approx 8.1$ meV	[91]
	$A_2 \approx 6.9$ meV		$A_2 \approx 1.1$ meV	

7.1. Co/Cu(001)/Co

The Co/Cu(001)/Co system is the one which has been most investigated theoretically and it is considered to be a model system for testing the predictions of theory. The theoretical results reported in table 3 correspond to semi-infinite magnetic layers, whereas the experimental data have been obtained for magnetic layers of finite thickness. As discussed in section 5, the strength of the coupling varies with the magnetic layer thickness, which can be a source of discrepancy between theoretical an experimental results. Another possible source of discrepancy is the unavoidable imperfection (roughness, intermixing) of the experimental samples.

Let us first address the short-period oscillatory component (labelled with the subscript 1). As discussed in section 4 above, this component arises from four equivalent in-plane wavevectors $\boldsymbol{k}_{\parallel 1}$ located on the $\overline{\Gamma}$–$\overline{\mathrm{X}}$ high-symmetry line of the two-dimensional Brillouin zone [36]. Since the majority-spin band structure of fcc Co matches well that of Cu, one has $|r_1^{\uparrow}| \approx 0$. On the other hand, for minority-spin fcc Co, there is a local gap in the band structure of symmetry compatible with the Cu states, which leads to total reflection, i.e., $|r_1^{\downarrow}| = 1$. Thus, one has $|\Delta r_1| \approx 0.5$ [42, 114] and $|\Delta r_1|$ is (almost) independent of the Co thickness (reference [105]). The various theoretical values for the amplitude A_1 listed in table 3 agree

† Note that, in order to be able to compare various theoretical results with each other, we included in the present discussion only the calculations pertaining to semi-infinite magnetic layers.

rather well with each other, except the one from reference [115] which is almost a factor of 2 larger than the values obtained by other authors [105, 114, 116]. This discrepancy may be due to an error in the estimation of the curvature radius κ_1 of the Fermi surface, and of the Fermi velocity $v_{\perp 1}$, which are quite tricky to obtain accurately for $\boldsymbol{k}_{\parallel 1}$.

Turning now to the comparison between theory and experiment, we notice that the calculated values of A_1 are considerably larger than the measured ones. At least two factors can contribute to this discrepancy. The first one is the effect of interface roughness, which generally tends to reduce the amplitude of the coupling oscillations [33]; this effect is particularly pronounced for short-period oscillatory components, as is indeed confirmed experimentally [87]. The second factor is of intrinsic character: the theoretical values of A_1 given in table 3 correspond to the asymptotic limit, whereas the experimental data have been obtained for spacer thicknesses below 15 AL. As is clearly apparent from figure 6(a) of reference [105] and from figure 13 (bottom) of reference [116], the asymptotic regime is attained only for thicknesses above 20 to 40 AL; below, the envelope of the oscillations deviates significantly from a D^{-2}-behaviour, and the apparent amplitude in the range relevant to experiments is typically a factor of 2 smaller than the asymptotic amplitude. This pre-asymptotic correction is attributed to a strong energy dependence of $r_1^{\downarrow}$ (reference [116]).

Let us now discuss the long-period oscillatory component. As is apparent from table 3, the situation is quite confusing: not only do the various theoretical results disagree with each other, but also some of them [114–116] *underestimate* the coupling strength as compared to the experiment [40, 85, 86], a fact which cannot be explained by the effect of roughness or interdiffusion.

The long-period oscillatory component arises from the centre $\overline{\Gamma}$ of the two-dimensional Brillouin zone. Here again, for the same reason as above, one has $|r_2^{\uparrow}| \approx 0$. The minority-spin reflection coefficient, on the other hand, is considerably smaller than for the short-period oscillation, and one has $|r_2^{\downarrow}| \approx 0.15$ [36], so $|\Delta r_2| \approx 0.05$ [36, 114]. This very small spin-dependent confinement explains the very small values of A_2 obtained by the authors who rely on the asymptotic expression (27) obtained from the stationary-phase approximation [114–116]. However, as seen from figure 2 of reference [118] and figure 2 of reference [115], $r_2^{\downarrow}$ increases very strongly with $\boldsymbol{k}_{\parallel}$ and full reflection is reached at a distance $0.1 \times \pi/a$ from $\overline{\Gamma}$; indeed, the low reflectivity arises only in a narrow window around $\overline{\Gamma}$. As discussed in reference [119], this gives rise to a strong pre-asymptotic correction, and explains why the stationary-phase approximation yields an *underestimated* value of A_2. On the other hand, if the $\boldsymbol{k}_{\parallel}$-integration is performed without using the stationary-phase approximation, as was done in reference [105], a much higher value of A_2 is obtained; the latter is larger than the experimental one [40, 85, 86] by a factor of 2.5, which seems plausible in view of the effect of roughness and interdiffusion.

Our knowledge of the phase of the oscillations is much more restricted, as this aspect of the problem has attracted little attention so far, with the notable exception of the work of Weber *et al* [87]. On general grounds, in the case of total reflection (as is the case for $r_{1\downarrow}$), one expects the phase to vary with magnetic layer thickness and/or with the chemical nature of the magnetic layer; conversely, for a case of weak confinement (such as that for $r_2^{\downarrow}$), one expects the phase to be almost invariant [36]. These general trends are indeed confirmed experimentally by Weber *et al* [87].

7.2. Fe/Au(001/Fe

The system Fe/Au(001)/Fe is actually an excellent system for a quantitative test of the theory. This is due to the excellent lattice matching between Au and bcc Fe (rotating the cubic axes of the latter by 45°), and to the availability of extremely smooth Fe substrates (whiskers) [90, 91].

In contrast to the Co/Cu(001) case discussed above, for Fe/Au(001), one has total reflection of minority-spin electrons both at $\boldsymbol{k}_{\parallel 1}$ (short-period oscillation) and $\boldsymbol{k}_{\parallel 2}$ (long-period oscillation), and $|r^{\downarrow}|$ is almost independent of $\boldsymbol{k}_{\parallel}$ around these points, as is clearly apparent from figure 1 of reference [42]. Therefore, the associated pre-asymptotic correction should not be very strong.

Indeed, as is seen from table 3, the predicted amplitudes are quite large, both for the short-period and long-period oscillatory components (reference [115]). These predictions are fairly well confirmed by state-of-the-art experimental studies [91], although the predicted amplitude of the long-period component is too large by a factor of 6.

Clearly, even for this almost ideal system, further work is required to achieve a satisfactory quantitative agreement between theory and experiment.

8. Concluding remarks

As has been discussed in detail in this review, there is a great deal of experimental evidence that the mechanism of quantum confinement presented above is actually the appropriate one to explain the phenomenon of oscillatory interlayer exchange coupling. This mechanism is entirely based upon a picture of independent electrons. This may seem paradoxical at first sight, in view of the fact that exchange interactions are ultimately due to the Coulomb interaction between electrons. In fact, this independent-electron picture can be justified theoretically and is based upon the 'magnetic force theorem.' A thorough discussion of this fundamental (but somewhat technical) aspect of the problem is given elsewhere [120, 121].

In spite of the successes encountered by the quantum confinement mechanism, a number of questions remain to be clarified for a full understanding of the phenomenon. In particular, one needs to assess in a more quantitative manner than has been achieved so far the validity of the asymptotic expression (27); a first attempt towards addressing this issue is given in reference [119].

Acknowledgments

I am grateful to Claude Chappert, Josef Kudrnovský, Vaclav Drchal and Ilja Turek for their collaboration on the work presented in this paper.

References

[1] Grünberg P, Schreiber R, Pang Y, Brodsky M B and Sowers C H 1986 *Phys. Rev. Lett.* **57** 2442
[2] Parkin S S P, More N and Roche K P 1990 *Phys. Rev. Lett.* **64** 2304
[3] Parkin S S P 1991 *Phys. Rev. Lett.* **67** 3598
[4] Toscano S, Briner B, Hopster H and Landolt M 1992 *J. Magn. Magn. Mater.* **114** L6
[5] Mattson J E, Kumar S, Fullerton E E, Lee S R, Sowers C H, Grimditch M, Bader S D and Parker F T 1993 *Phys. Rev. Lett.* **71** 185
[6] Briner B and Landolt M 1994 *Phys. Rev. Lett.* **73** 340
[7] Bruno P 1994 *Phys. Rev.* B **49** 13 231
[8] Inomata K, Yusu K and Saito Y 1995 *Phys. Rev. Lett.* **74** 1863
[9] de Vries J J, Kohlhepp J, den Broeder F J A, Verhaegh P A, Jungblut R, Reinders A and de Jonge W J M 1997 *J. Magn. Magn. Mater.* **165** 435
[10] Rührig M, Schäfer R, Hubert A, Mosler R, Wolf J A, Demokritov S and Grünberg P 1991 *Phys. Status Solidi* a **125** 635
[11] Demokritov S, Wolf J A, Grünberg P and Zinn W 1991 *Magnetic Surfaces, Thin Films and Multilayers Symp.* ed S S P Parkin *et al* (Pittsburgh, PA: Materials Research Society) p 133
[12] Unguris J, Celotta R J and Pierce D T 1991 *Phys. Rev. Lett.* **67** 140

[13] Unguris J, Celotta R J and Pierce D T 1992 *Phys. Rev. Lett.* **69** 1125
[14] Wolf J A, Leng Q, Schreiber R, Grünberg P, Zinn W and Schuller I K 1993 *J. Magn. Magn. Mater.* **121** 253
[15] Fullerton E E, Conover M J, Mattson J E, Sowers C H and Bader S D 1993 *Phys. Rev.* B **48** 15 755
[16] Fullerton E E, Riggs K T, Sowers C H, Bader S D and Berger A 1995 *Phys. Rev. Lett.* **75** 330
[17] Meerschaut J, Dekoster J, Schad R, Beliën P and Rots M 1995 *Phys. Rev. Lett.* **75** 1638
[18] Schreyer A, Ankner J F, Zeidler T, Zabel H, Schäfer R, Wolf J A, Grünberg P and Majkrzak C F 1995 *Phys. Rev.* B **52** 16 066
[19] Fullerton E E, Bader S D and Robertson J L 1996 *Phys. Rev. Lett.* **77** 1382
[20] Grimditch M, Kumar S and Fullerton E E 1996 *Phys. Rev.* B **54** 3385
[21] Schreyer A, Majkrzak C F, Zeidler T, Schmitte T, Bödeker P, Theis-Bröhl K, Abromeit A, Dura J and Watanabe T 1997 *Phys. Rev. Lett.* **79** 4914
[22] Majkrzak C F, Cable C W, Kwo J, Hong M, McWhan B D, Yafet Y, Waszcak J V and Vettier C 1986 *Phys. Rev. Lett.* **56** 2700
[23] Salamon M B, Sinha S, Rhyne J J, Cunningham J E, Erwin R W, Borchers J and Flynn C P 1986 *Phys. Rev. Lett.* **56** 259
[24] Majkrzak C F, Kwo J, Hong M, Yafet Y, Gibbs D, Chein C L and Bohr J 1991 *Adv. Phys.* **40** 99
[25] Rhyne J J and Erwin R W 1995 *Magnetic Materials* vol 8, ed K H J Buschow (Amsterdam: North-Holland) p 1
[26] Slonczewski J C 1995 *J. Magn. Magn. Mater.* **150** 13
[27] Demokritov S O 1998 *J. Phys. D: Appl. Phys.* **31** 925
[28] Bruno P, Kudrnovský J, Drchal V and Turek I 1996 *Phys. Rev. Lett.* **76** 4253
[29] Kudrnovský J, Drchal V, Bruno P, Turek I and Weinberger P 1996 *Phys. Rev.* B **54** 3738
[30] Bruno P, Kudrnovský J, Drchal V and Turek I 1997 *J. Magn. Magn. Mater.* **165** 128
[31] Drchal V, Kudrnovský J, Bruno P, Dederichs P H and Weinberger P 1998 *Phil. Mag.* B **78** 571
[32] Edwards D M, Mathon J, Muniz R B and Phan M S 1991 *Phys. Rev. Lett.* **67** 493
[33] Bruno P and Chappert C 1991 *Phys. Rev. Lett.* **67** 1602
Bruno P and Chappert C 1991 *Phys. Rev. Lett.* **67** 2592 (erratum)
[34] Bruno P 1993 *J. Magn. Magn. Mater.* **121** 248
[35] Stiles M D 1993 *Phys. Rev.* B **48** 7238
[36] Bruno P 1995 *Phys. Rev.* B **52** 411
[37] Fert A and Bruno P 1994 *Ultrathin Magnetic Structures* vol 2, ed B Heinrich and J A C Bland (Berlin: Springer) ch 2.2, p 82
[38] Yafet Y 1994 *Magnetic Multilayers* ed L H Bennett and R E Watson (Singapore: World Scientific) p 19
[39] Fert A, Grünberg P, Barthélémy A, Pétroff F and Zinn W 1995 *J. Magn. Magn. Mater.* **140–144** 1
[40] de Vries J J 1996 *PhD Thesis* Eindhoven University of Technology
[41] Jones B A 1998 *IBM J. Res. Dev.* **42** 25
[42] Stiles M D 1999 *J. Magn. Magn. Mater.* **200** 322
[43] Loly P D and Pendry J B 1983 *J. Phys. C: Solid State Phys.* **16** 423
[44] Wachs A L, Shapiro A P, Hsieh T C and Chiang T-C 1986 *Phys. Rev.* B **33** 1460
[45] Lindgren S Å and Walldén L 1987 *Phys. Rev. Lett.* **59** 3003
[46] Lindgren S Å and Walldén L 1988 *Phys. Rev. Lett.* **61** 2894
[47] Lindgren S Å and Walldén L 1988 *Phys. Rev.* B **38** 3060
[48] Lindgren S Å and Walldén L 1989 *J. Phys.: Condens. Matter* **1** 2151
[49] Miller T, Samsavar A, Franklin G E and Chiang T-C 1988 *Phys. Rev. Lett.* **61** 1404
[50] Mueller M A, Samsavar A, Miller T and Chiang T-C 1989 *Phys. Rev.* B **40** 5845
[51] Mueller M A, Miller T and Chiang T-C 1990 *Phys. Rev.* B **41** 5214
[52] Jałochowski M, Bauer E, Knoppe H and Lilienkamp G 1992 *Phys. Rev.* B **45** 13 607
[53] Brookes N B, Chang Y and Johnson P D 1991 *Phys. Rev. Lett.* **67** 354
[54] Ortega J E and Himpsel F J 1992 *Phys. Rev. Lett.* **69** 844
[55] Ortega J E, Himpsel F J, Mankey G J and Willis R F 1993 *Phys. Rev.* B **47** 1540
[56] Ortega J E, Himpsel F J, Mankey G J and Willis R F 1993 *J. Appl. Phys.* **73** 5771
[57] Garrison K, Chang Y and Johnson P D 1993 *Phys. Rev. Lett.* **71** 2801
[58] Carbone C, Vescovo E, Rader O, Gudat W and Eberhardt W 1993 *Phys. Rev. Lett.* **71** 2805
[59] Smith N V, Brookes N B, Chang Y and Johnson P D 1994 *Phys. Rev.* B **49** 332
[60] Johnson P D, Garrison K, Dong Q, Smith N V, Li D, Mattson J E, Pearson J and Bader S D 1994 *Phys. Rev.* B **50** 8954
[61] Himpsel F J and Rader O 1995 *Appl. Phys. Lett.* **67** 1151
[62] Crampin S, De Rossi S and Ciccaci F 1996 *Phys. Rev.* B **53** 13 817

[63] Segovia P, Michel E G and Ortega J E 1996 *Phys. Rev. Lett.* **77** 3455
[64] Kläsges R, Schmitz D, Carbone C, Eberhardt W, Lang P, Zeller R and Dederichs P H 1998 *Phys. Rev.* B **57** R696
[65] Kawakami R K, Rotenberg E, Escocia-Aparicio E J, Choi H J, Cummins T R, Tobin J G, Smith N V and Qiu Z Q 1998 *Phys. Rev. Lett.* **80** 1754
[66] Kawakami R K, Rotenberg E, Escocia-Aparicio E J, Choi H J, Wolfe J H, Smith N V and Qiu Z Q 1999 *Phys. Rev. Lett.* **82** 4098
[67] Himpsel F J 1991 *Phys. Rev.* B **44** 5966
[68] Ortega J E and Himpsel F J 1993 *Phys. Rev.* B **47** 16 441
[69] Li D, Pearson J, Mattson J E, Bader S D and Johnson P D 1995 *Phys. Rev.* B **51** 7195
[70] Himpsel F J 1995 *J. Electron Microsc. Relat. Phenom.* **75** 187
[71] Li D, Pearson J, Bader S D, Vescovo E, Huang D-J, Johnson P D and Heinrich B 1997 *Phys. Rev. Lett.* **78** 1154
[72] Koike K, Furukawa T, Cameron G P and Murayama Y 1994 *Phys. Rev.* B **50** 4816
[73] Furukawa T and Koike K 1996 *Phys. Rev.* B **54** 17 896
[74] Bennett W R, Schwarzacher W and Egelhoff W F Jr 1990 *Phys. Rev. Lett.* **65** 3169
[75] Katayama T, Suzuki Y, Hayashi M and Thiaville A 1993 *J. Magn. Magn. Mater.* **126** 527
[76] Carl A and Weller D 1995 *Phys. Rev. Lett.* **74** 190
[77] Mégy R, Bounouh A, Suzuki Y, Beauvillain P, Bruno P, Chappert C, Lécuyer B and Veillet P 1995 *Phys. Rev.* B **51** 5586
[78] Bruno P, Suzuki Y and Chappert C 1996 *Phys. Rev.* B **53** 9214
[79] Suzuki Y, Katayama T, Bruno P, Yuasa S and Tamura E 1998 *Phys. Rev. Lett.* **80** 5200
[80] Luce T A, Hübner W and Bennemann K H 1996 *Phys. Rev. Lett.* **77** 2810
[81] Kirilyuk A, Rasing T, Mégy R and Beauvillain P 1996 *Phys. Rev. Lett.* **77** 4608
[82] Weber W, Bischof A, Allenspach R, Würsch C, Back C H and Pescia D 1996 *Phys. Rev. Lett.* **76** 3424
[83] Back C H, Weber W, Würsch C, Bischof A, Pescia D and Allenspach R 1997 *J. Appl. Phys.* **81** 5054
[84] Halse M R 1969 *Phil. Trans. R. Soc.* A **265** 507
[85] Johnson M T, Purcell S T, McGee N W E, Coehoorn R, aan de Stegge J and Hoving W 1992 *Phys. Rev. Lett.* **68** 2688
[86] Johnson M T, Bloemen P J H, Coehoorn R, de Vries J J, McGee N W E, Jungblut R, Reinders A and aan de Stegge J 1993 *Mater. Res. Soc. Symp. Proc.* **313** 93
[87] Weber W, Allenspach R and Bischof A 1995 *Europhys. Lett.* **31** 491
[88] Unguris J, Celotta R J and Pierce D T 1993 *J. Magn. Magn. Mater.* **127** 205
[89] Fuss A, Demokritov S, Grünberg P and Zinn W 1992 *J. Magn. Magn. Mater.* **103** L221
[90] Unguris J, Celotta R J and Pierce D T 1994 *J. Appl. Phys.* **75** 6437
[91] Unguris J, Celotta R J and Pierce D T 1997 *Phys. Rev. Lett.* **79** 2734
[92] Mosca D H, Pétroff F, Fert A, Schroeder P A, Pratt W P Jr, Laloee R and Lequien S 1991 *J. Magn. Magn. Mater.* **94** L1
[93] Schreyer A, Bröhl K, Ankner J F, Majkrzak, C F, Zeidler T, Bödeker P, Metoki N and Zabel H 1993 *Phys. Rev.* B **47** 15 334
[94] Pétroff F, Barthélémy A, Mosca D H, Lottis D K, Fert A, Schroeder P A, Pratt W P Jr, Laloee R and Lequien S 1991 *Phys. Rev.* B **44** 5355
[95] de Miguel J J, Cebollada A, Gallego J M, Miranda R, Schneider C M, Schuster P and Kirschner J 1991 *J. Magn. Magn. Mater.* **93** 1
[96] Okuno S N and Inomata K 1993 *Phys. Rev. Lett.* **70** 1771
[97] Parkin S S P, Chappert C and Herman F 1993 *Europhys. Lett.* **24** 71
[98] Bobo J-F, Hennet L and Piécuch M 1993 *Europhys. Lett.* **24** 139
[99] Bruno P 1993 *Europhys. Lett.* **23** 615
[100] Barnaś J 1992 *J. Magn. Magn. Mater.* **111** L215
[101] Bloemen P J H, Johnson M T, van de Vorst M T H, Coehoorn R, de Vries J J, Jungblut R, aan de Stegge J, Reinders A and de Jonge W J M 1994 *Phys. Rev. Lett.* **72** 764
[102] Back C H, Weber W, Bischof A, Pescia D and Allenspach R 1995 *Phys. Rev.* B **52** R13 114
[103] Nordström L, Lang P, Zeller R and Dederichs P 1994 *Phys. Rev.* B **50** 13 058
[104] Lang P, Nordström L, Wildberger K, Zeller R, Dederichs P and Hoshino T 1996 *Phys. Rev.* B **53** 9092
[105] Drchal V, Kudrnovský J, Turek I and Weinberger P 1996 *Phys. Rev.* B **53** 15 036
[106] Lee B and Chang Y-C 1996 *Phys. Rev.* B **54** 13 034
[107] Bruno P 1996 *J. Magn. Magn. Mater.* **164** 27
[108] de Vries J J, Schudelaro A A P, Jungblut R, Bloemen P J H, Reinders A, Kohlhepp J, Coehoorn R and de Jonge W J M 1995 *Phys. Rev. Lett.* **75** 1306

[109] Okuno S N and Inomata K 1995 *J. Phys. Soc. Japan* **64** 3631
[110] Bounouh A, Beauvillain P, Bruno P, Chappert C, Mégy M and Veillet P 1996 *Europhys. Lett.* **33** 315
[111] Kudrnovský J, Drchal V, Bruno P, Turek I and Weinberger P 1997 *Phys. Rev.* B **56** 8919
[112] Kudrnovský J, Drchal V, Bruno P, Coehoorn R, de Vries J J and Weinberger P 1997 *Mater. Res. Soc. Symp. Proc.* **475** 575
[113] Kudrnovský J, Drchal V, Bruno P, Turek I and Weinberger P 1998 *Comput. Mater. Sci.* **10** 188
[114] Lee B and Chang Y-C 1995 *Phys. Rev.* B **52** 3499
[115] Stiles M D 1996 *J. Appl. Phys.* **79** 5805
[116] Mathon J, Villeret M, Umerski A, Muniz R B, d'Albuquerque e Castro J and Edwards D M 1997 *Phys. Rev.* B **56** 11 797
[117] Ives A J R, Hicken R J, Bland J A C, Daboo C, Gester M and Gray S J 1994 *J. Appl. Phys.* **75** 6458
[118] Bruno P 1995 *J. Magn. Magn. Mater.* **148** 202
[119] Bruno P 1999 *Eur. Phys. J.* B **11** 83
[120] Bruno P 1999 *Magnetische Schichtsysteme* ed P H Dederichs and P Grünberg (Jülich: Forschungszentrum) ch B8
Bruno P 1999 *Preprint* cond-mat/9905022
[121] Bruno P 1999 to be published